Exploration of conformational switching in Aβ16–22 peptide analogues via Molecular dynamics simulations

Kanchan Yadav, Gopal Singh Bisht, and Tiratha Raj Singh#*
Jaypee University of Information Technology, Waknaghat, Solan, Himachal Pradesh
173234. Department of Biotechnology and Bioinformatics
*gopal.singh@juitsolan.in; #tiratharaj.singh@juitsolan.in

Abstract

Neurodegenerative disorders (ND) such as Alzheimer's (AD) remain a major incurable problem largely due to an opaque mechanistic understanding of pathogenic protein aggregation at the molecular level. While amyloid beta (Aβ) fibrils are the main culprits in AD pathology, recent evidence indicates that early oligomers are neurotoxic. The K16-E22 hydrophobic core governs β-sheet formation, cross-seeding interactions with tau, and nucleation kinetics, thereby regulating Aβ conformational switching. In this study, a rational peptide-analogue strategy was adopted to explore how sequence-level mutations within the K16-E22 segment regulate conformational stability and aggregation. Initially, 18 peptide analogues were designed and screened using PROTPARAM (hydrophobicity) and WALTZ (beta-propensity). Following the evaluation of these metrics, five representative analogues were selected to systematically evaluate specific molecular attributes such as enhanced hydrophobicity (ALVFFAE: GRAVY +1.957, WALTZ 98.66), increased β-propensity (KIVFFAE: GRAVY +1.243, WALTZ 98.327), β-sheet disruption via proline insertion (KLPFFAE: GRAVY +0.314, WALTZ 0), charge density effects (KKVFFAE: GRAVY +0.043, WALTZ 0), and positional charge redistribution without hydrophobicity change (LVFKFAE: GRAVY +1.143, WALTZ 94.31), using the native KLVFFAE (GRAVY +1.143, WALTZ 97.8) sequence as a control. Three-dimensional structures of these selected peptides were generated using PEP-FOLD and validated using QMEAN scores before molecular dynamics (MD) simulations (GROMACS) to link sequence properties to conformational switching pathways. This work aims to pinpoint which molecular feature drives peptide aggregation and which helps them resist it. The results of this study are hypothesized to illuminate mechanistic details of disease progression and to enable the rational design of peptide-based aggregation modulators.

Keywords: neurodegenerative disorders (ND), Alzheimer's disease (AD), amyloid beta (Aβ), in silico analysis, conformational switching, hydrophobicity, hydrophobic collapse.

1. Introduction

Alzheimer's disease is regarded as a progressively fatal neurodegenerative disorder and the leading cause of dementia, cognitive decline, etc., worldwide. Dementia currently affects over 55 million people globally, of whom approximately 60-70% people are suffering from AD[1]. Even though all neurodegenerative disorders collectively are a growing global health care challenge, AD still remains a major burden on the health care system due to its high prevalence, long disease duration that requires constant care, and multisystem implications. Recent evidence supports the existence of certain pathophysiological links between AD and other metabolic conditions, such as type 2 diabetes mellitus, as shown in the paper by N. Cramer et al., which proposes a mechanistic understanding of amyloid-β (Aβ) and islet amyloid polypeptide (IAPP) cross-seeding interactions [2].

The accumulation of Aβ peptides in the brain is a feature of AD. This mechanism of aggregation is a multi-step kinetic reaction with the following stages. The initial phase is the lag phase, during which the main form of Aβ is monomeric. This is followed by slow primary nucleation, in which monomers spontaneously assemble into small, unstable, and reversible aggregates driven by electrostatic and hydrophobic forces to form oligomers. Following this is the exponential growth phase, which is characterized by rapid fibril elongation and secondary nucleation. These fibrils can then assist in the formation of new oligomers through secondary nucleation. Only the oligomeric species that are stable can convert into fibrillar structures, which elongate with the addition of more monomers. Finally, there is the saturation phase, in which fibril elongation is limited by monomer depletion. But via fibril fragmentation during this stage, an increase in small fibrillar species is seen, generating elongation-competent ends[3,5]. Given the role of neurotoxic oligomers formed from Aβ42 monomers in the pathogenesis of AD, the current research aims to determine approaches to suppress the formation and subsequent progression of oligomeric forms[4].

The primary aim of this research is to understand the mechanistic aspects of Aβ oligomer formation, focusing on the conformational transformations of monomers into oligomers that are likely to form aggregates. Now, these types of conformational switches have reportedly been observed in various amyloidogenic proteins; they are driven by both extrinsic and intrinsic factors [6]. While extrinsic factors such as pH, temperature, and ionic strength significantly regulate a protein's structure and aggregation behaviour, our present study focuses more on the role of intrinsic factors [6]. We specifically investigate how sequence-level disturbances that alter the physicochemical properties of the sequence, such as hydrophobicity or β-sheet propensity, can also affect the conformational transition from a random coil to β-strand-rich aggregates.

Despite current research focusing on understanding the mechanistic details of Aβ aggregation, the role of sequence-level intrinsic factors in driving conformational switching remains incompletely understood [7]. In particular, the comparative influences of hydrophobicity and β-propensity on structural rearrangement in APR regions are emerging as a major challenge. Currently, researchers such as Lorena Roldán-Martín et al. have hypothesized that mutations centred on the segment K16-E22 of Aβ42 can have a drastic effect on the physicochemical parameters and aggregation behaviour [7].

We rationally engineered peptide analogues of the main segment (KLVFFAE) to test this hypothesis, by altering the amino acid composition of the sequence that influences the hydrophobicity, β-propensity and charge of the native segment and then carried out MD simulations to elucidate the inherent factors in the conformational switching and oligonucleation. This segment of Aβ42 has been widely recognized as a prime core for driving conformational switch in neurotoxic species.

2. Methodology

2.1 Sequence Design

As mentioned above, the central hydrophobic core region (KLVFFAE) of Aβ42 plays an important role in oligomer and fibril formation. Corresponding aggregation-prone regions (APRs) have been reported in other amyloidogenic proteins[3], such as regions that are frequently concealed in the hydrophobic core of a native protein and are revealed during denaturation or partial unfolding. The exposure of such regions has been shown to assist oligomer formation. The APR regions exhibit high hydrophobicity and β-sheet propensity, favoring the formation and aggregation into β-strands [3].

Efforts have been made over last few years to come up with a number of computational tools that can be used to identify the APRs of a protein, an enzyme or a longer peptide. In this work, WALTZ was used to assess amyloidogenic propensity, whereas **Protparam** and **Protscale** were used to assess hydrophobicity. We used these tools as preliminary screening filters to rationally design peptide analogues of the original segment (KLVFFAE) and then select 5 representative peptide analogues from the list.

Therefore, based on systematic sequence modifications of the Aβ42 K16–E22 segment (KLVFFAE), multiple peptide analogues were generated and presented in the table below. From these, 5 representative peptides were selected and grouped as: enhancer, blocker, equivalence, charge variant, and β-propensity control. Selection criteria for representative peptide analogues were based on relative hydrophobicity, β-propensity and charge distribution.

Table 1: Rationally designed peptide analogues with highlighted selected representative peptides (marked bold)

Peptide Analogue	GRAVY	WALTZ	PI	MW
KWVFFAE	0.471	94.31	6	926.08
KAVFFAE	0.857	97.99	6	810.95
KIVFFAE	1.243	98.327759	6	853
KLVFFWE	0.757	93.16770134	6	968
KLVFFAW	1.514	97.993311	8.75	910
KLVFFAT	1.543	97.993311	8.75	825
KLVFFAV	2.243	97.993311	8.75	823
ILVFFAE	2.343	98.327759	4	838
FLVFFAE	2.1	98.327759	4	872
KLPFFAE	0.314	NIL	6	851
ALVFFAE	1.957	98.662207	4	795
KLVPFAE	0.154	NIL	6	802
KLVFPAE	0.154	NIL	6	802
KLVFFPE	0.657	NIL	6	879
KKVFFAE	0.043	NIL	8.59	868
LVKFFAE	1.143	NIL	6	853
LVFKFAE	1.143	94.314381	6	853

The following information is about the chosen representative peptides. Peptide 1 (KKVFFAE) has been classified as a charge variant, with an additional lysine residue, resulting in a greater positive charge. Then, peptide 2 (KIVFFAE) was categorized as a β-propensity control, showing high β-propensity (98.9%) due to the isoleucine substitution. There is peptide 3 (KLPFFAE), which is categorized as a blocker owing to its proline, a β-strand breaker. Following this is peptide 4 (ALVFFAE) placed as an enhancer, expressing the highest hydrophobicity (1.957) and equally higher β propensity (98.66%), and lastly peptide 5 (LVFKFAE) categorized as equivalence, with its hydrophobicity (1.143) and β propensity (94.3%) very in line with that of the native KLVFFAE segment.

The working hypothesis was that the enhancer peptide (peptide 4) would express accelerated aggregation relative to the equivalence peptide (peptide 5), whereas the blocker (peptide 3) and charge variant peptide (peptide 1), would inhibit β-strand formation due to the presence of proline or due to charge repulsion, respectively. Conversely, β-propensity control peptide (peptide 2) was made in order to establish whether the presence, by itself, of increased β propensity is sufficient to control aggregation behaviour. A key consideration is that WALTZ and ProtScale analyses were used as preliminary screening tools to support rational peptide selection [8]. Now, to prove this hypothesis, the structures of these peptides were downloaded from PEP-FOLD and model quality was assessed using QMEAN scoring via the SWISS-MODEL server. The subsequent molecular dynamics simulations were performed to test these hypotheses and assess aggregation-related conformational behaviour [8].

2.2 MD Setup

MD simulations apply physics-based potential energy functions (called force fields) to model the motion of biomolecules, mostly proteins, over time according to classical Newtonian mechanics[6]. Despite the valuable insights provided by WALTZ, ProtScale, and PDB on the physicochemical properties and aggregation propensity of proteins, they lack the spatial and temporal resolution required to directly observe conformational transitions [8].

That's where MD simulation comes into play; it provides atomistic detail of structural rearrangements and dynamic intermolecular interactions that are difficult to capture experimentally, even with techniques like NMR or CD spectroscopy [6]. Building on the sequence screening analysis, MD simulations were performed using the GROMACS simulation package, which has been deemed one of the most widely used open-source software packages for biomolecular simulations[9]. GROMACS has a broad range of system preparation, integration, and trajectory analysis tools, which is why it is applicable to the investigation of peptide conformational dynamics and aggregation behaviour [9].

2.3 Simulation Protocol

All the peptides were first simulated in their monomeric form for 5 ns, followed by simulations under oligomeric conditions. For both monomer and oligomer simulations, the following parameters were applied: force field (AMBER99SB-ILDN), water model (SPC/E), pressure coupling (Parrinello–Rahman barostat), electrostatics (Particle Mesh Ewald (PME) method), constraints: LINCS algorithm applied to bonds involving hydrogen atoms, and boundary conditions (Periodic boundary conditions in all three spatial directions).

We selected the AMBER99SB-ILDN force field because it provides better side-chain torsion parameterisation, optimizing the accuracy with which peptide conformational behaviour is modelled and aggregation-related transitions are refined [7]. The SPC/E water model was chosen because it offers enhanced dielectric properties and diffusion behaviour compared to the simplistic three-point model and was thus suitable for simulations where dielectric-controlled interactions are key [10].

Simulation time and system composition were the major differences between the monomeric and oligomeric simulations. Monomer simulations consisted of a single 7-residue peptide chain and were run for 5 ns. Oligomeric simulations spanned 20 ns and included 10 peptide chains within the simulation box. The monomer timescale was sufficient to capture early conformational fluctuations and assess sequence-dependent conformational rearrangements; alternatively, the longer simulation time of 20 ns for the oligomeric run was required to observe the intermolecular interactions, hydrophobic collapse and early aggregation events in multi-chain systems[2].

Simulations of monomers were carried out prior to oligomer simulations to determine whether the properties of single-residue substitutions within the K16-E22 hydrophobic core influence the intrinsic conformational stability of individual peptide chains[2]. This step validated the aggregation propensity prediction of WALTZ; later oligomer simulations were performed to determine whether these sequence-level modifications shaping monomer conformational behaviour would translate into altered aggregation propensity and intermolecular assembly dynamics[6]. The broader exploration of this work-flow is that knowledge of sequence-driven conformational determinants can be used as part of rational design approaches to aggregation inhibitors, if they are designed to reduce initial oligomer formation.

3. Results

3.0 Model Validation

Prior to MD results, peptide models downloaded from PEP-FOLD were evaluated using QMEAN scoring to assess their structural reliability and to establish a baseline for conformational analysis.

Table 2: QMEAN scores of peptide analogues(1-5)

Peptide	QMEAN score
1	-4.67
2	-3.10

3	-1.46
4	-5.51
5	-5.51

The QMEAN scores varied across analogues, with peptide 3 showing the highest reliability (- 1.46), while peptides 4 and 5 exhibited lower reliability (- 5.51). Peptides 1 and 2, on the other hand, gave intermediate reliability scores of (-4.67 and -3.10 respectively). The purpose of these scores is not only to indicate the model quality but also to frame succeeding conformational dynamics. Peptides with lower-scoring models exhibit greater structural variability, whereas higher-scoring models provide more stable starting points for simulations. Thus, QMEAN aided as an initial predictor of conformational trends, guiding the interpretation of Ramachandran plots, RMSD and Rg trajectories in monomer simulations.

3.1 Monomer Stability

To begin with, monomeric simulations were conducted to test the conformational changes of peptide analogues; these simulations were performed initially because Aβ monomers are generally considered basic building blocks of aggregation and oligomerisation [6]. They have been demonstrated to react with larger oligomers and fibrils, and, as a result of these reactions, they play a role in the nucleation process and the formation of pathogenic dimers[5].

When cleaved by gamma-secretase, Aβ alters its conformation, forming a helical structure that is then transformed into disordered forms, eventually becoming β-rich. This conformational switch provides evidence for the aggregation pathway and underscores the importance of monomers in regulating oligomerisation and fibril formation [5].

To determine how the K16-E22 segment affects monomer stability and conformational changes, MD simulations were conducted for each representative peptide analogue. Root-mean-square deviation (RMSD), radius of gyration (Rg), and the Ramachandran plot were used to analyse structural stability and conformational dynamics.

3.1.1 Aggregation Relevance

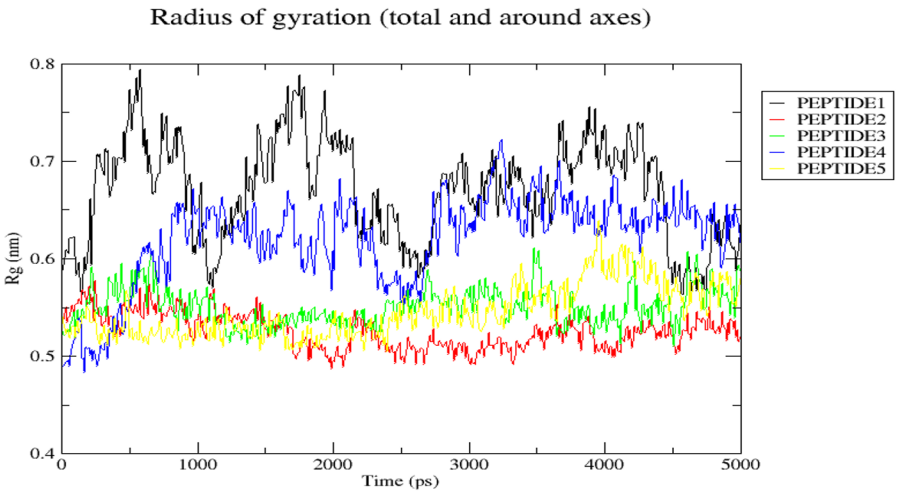

Figure 1: Radius of gyration plot for all the peptides (1-5) monomer simulation. This figure indicates Rg (nm) vs time (ps) of peptide 1 (black), peptide 2 (red), peptide 3 (green), peptide 4 (blue) and peptide 5 (yellow).

Constant trajectories are a sign of conformational compactness, whereas fluctuations are characteristics of structural flexibility and restructuring. All the peptides here maintain disordered states, with average Rg ranging from 0.45 to 0.79 nm, which is typical for short unfolded peptides (expected ~0.5-0.7 nm for 7-residue chains). There is no collapse or compaction; large variations indicate intermittent sampling of extended/compact conformers that do not fold steadily.

Peptides 1 (KKVFFAE) and 4 (ALVFFAE) exhibit substantial Rg variations, indicating substantial conformational rearrangements and decreased stability. Peptide 1 has the highest baseline of Rg (~0.79 nm), this suggests that it is the most extended and has maximum hydrophilic exposure. Peptide 4 has clear fluctuation at 1 ns from its initial conformation to another structural rearrangement, suggesting a conformational switch that will be seen later in oligomer simulation results. Peptide 5 (LVFKFAE) has a constant baseline Rg (~0.6-0.7 nm) with even oscillations, indicating that the peptide is moderately compact and possesses a moderate hydrophobic collapse propensity. Peptide 3 (KLPFFAE) exhibits mid-range oscillation with low Rg; the F3/F5/P6 facilitate the hydrophobic burial and thus compactness. Peptide 2 (KIVFFAE) has the lowest/most stable Rg (avg: ~0.45 nm), suggesting a compact, stable conformation throughout the simulation. Rg (radius of gyration) is used to determine the size and compactness of proteins by computing the distribution of atoms around the centre of mass; it is also used to monitor folding, unfolding, or structural stability in simulations.

The radius of gyration analysis of all the monomeric simulations of peptides 1, 2, 3, 4 and 5 revealed distinct stability profiles. Peptide 2 had the most stable conformation throughout the simulation. On the contrary, peptides 4 and 1 had the largest Rg values, with strong fluctuations, suggesting a tendency to expand their structures. The intermediate behaviour of peptides 3 and 5, with moderately compact structures and little conformational variability, was observed.

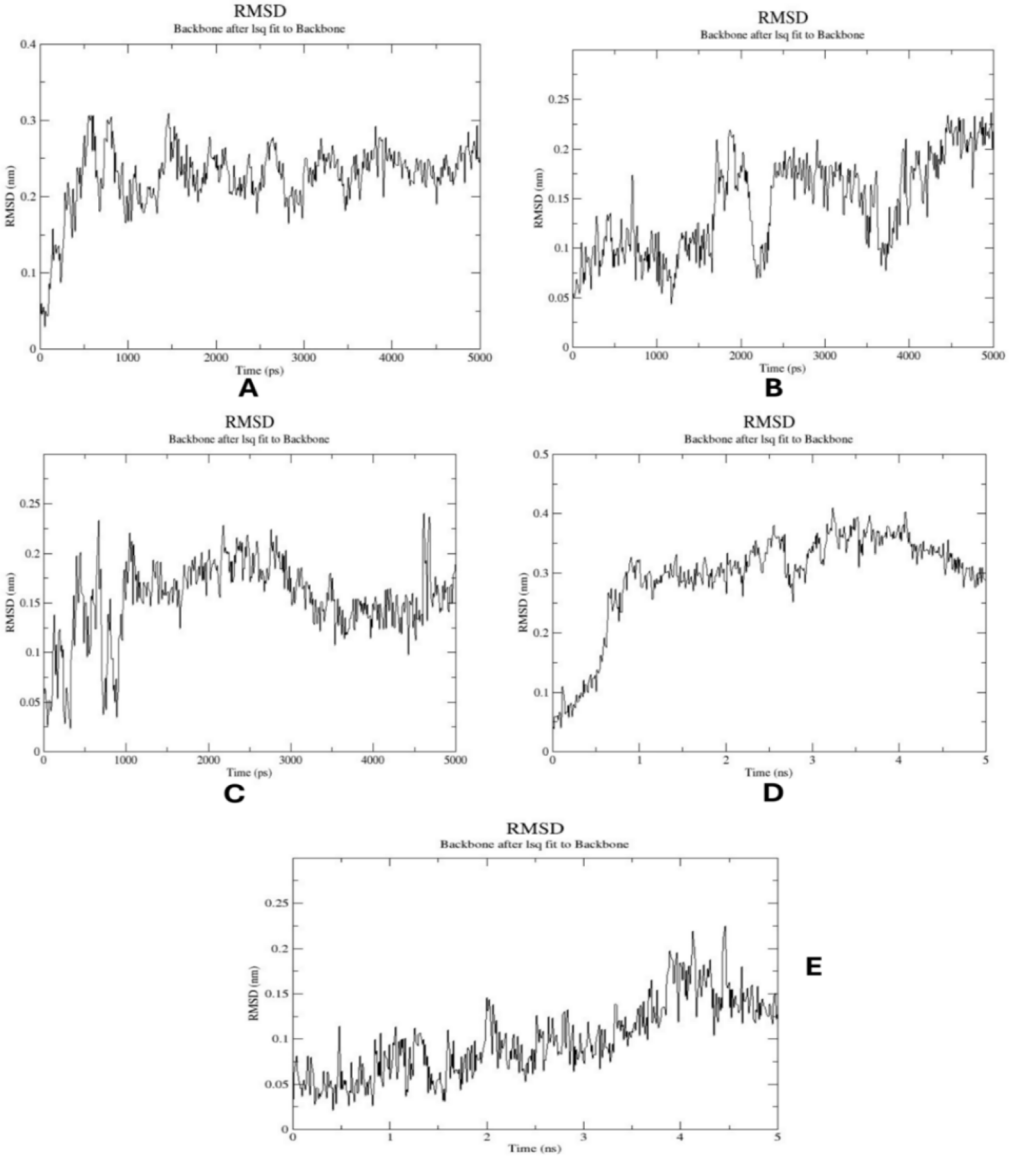

Figure 2: Monomeric peptides analogues backbone RMSD profiles of 5 ns MD simulations. (A) Peptide 1 (KKVFFAE), (B) Peptide 2 (KIVFFAE), (C) Peptide 3 (KLPFFAE), (D) Peptide 4 (ALVFFAE), (E) Peptide 5 (LVFKFAE).

Peptide 4 (ALVFFAE) exhibits the greatest structural deviation, consistent with its increased hydrophobic-driven conformational rearrangement behaviour, as seen in the Rg graph. Peptide 1 shows moderate flexibility, peptide 2 shows gradual RMSD increase from ~0.06 nm to ~0.2 nm indicating possible β structural sampling. Peptide 3 shows early fluctuation but later remains largely within ~0.12-0.20 nm. Peptide 5 behaves closest to a baseline control.

Increased hydrophobicity is associated with greater structural rearrangement in monomers in simulations. Nonetheless, a higher β propensity by itself (Peptide 2) fails to result in an equivalent extent of the structural deviation as a hydrophobic enhancement (Peptide 4). This helps in confirming our hypothesis that hydrophobic context and residue positioning are major roles in conformation switching. The peptide 2 plot B shows a compact distribution, indicating limited conformational sampling; this may be a form of stabilization via intermolecular hydrogen bonding or steric hindrance of the peptide backbone (due to the presence of Isoleucine). Conformational bistability can be observed in Plots C and D for peptides 3 and 4, with the appearance of distinct bands corresponding to alpha-helical and extended β-strand states.

The figure 3 of MD simulation results is an comparative analysis of Ramachandran plots of all 5 peptides in their monomeric forms over the span of 5ns. The aim of these Ramachandran plots was to give an emerging trend that these alpha helical and beta sheet arrangements of these peptide analogues will show potential conformational diversity.

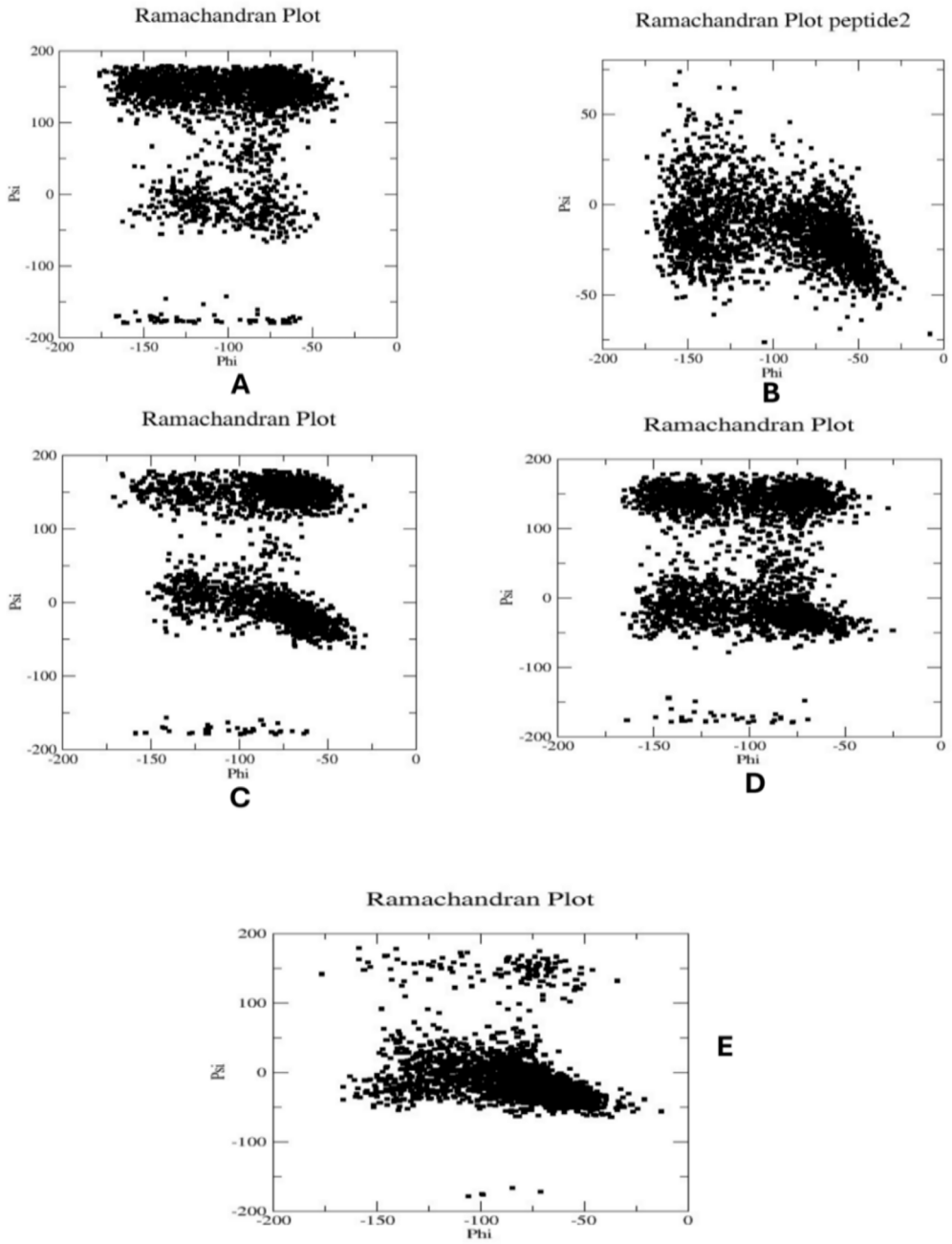

Figure 3: Ramachandran plots of monomeric peptide analogues over 5 ns MD simulations. (A-E) distribution of backbone dihedral angles (Φ, Ψ) for representative peptide simulations. (A) Peptide 1 (KKVFFAE), (B) Peptide 2 (KIVFFAE), (C) Peptide 3 (KLPFFAE), (D) Peptide 4 (ALVFFAE), and (E) Peptide 5 (LVFKFAE).

Plot D of peptide 4 shows predominant β-sheet conformations with scattered deviations, whereas Plot A of peptide 1 shows that due to increased electrostatic repulsion, the monomer remains structurally dynamic rather than adopting stable β-like conformations. Plot B of peptide 2 exhibits compact distribution, reflecting restricted conformational sampling; this could represent stabilization by intramolecular hydrogen bonding or steric constraints in the peptide backbone (due to isoleucine presence). Plots C and D of peptides 3 and 4 reveal distinct bands corresponding to α-helical ($\Psi \approx -45°$) and extended β strand ($\Psi \approx 150°$) states, highlighting conformational bistability within 5 ns. We note that these Ramachandran plots are derived from 5ns simulations, which are sufficient to capture early conformational fluctuations but may not fully sample the conformational variation of short peptides. Thus, observed α-helical and β-strand states should only be interpreted as emerging trends, with longer simulations potentially revealing additional conformational diversity.

3.2 Oligomer Aggregation

To evaluate oligomer compactness and hydrophobic collapse, the radius of gyration (Rg) was monitored over 20 ns simulations. Rg gives an idea about the total spatial distribution of the atoms in relation to the center of mass and is normally employed to determine structural compaction throughout aggregation, high frequency oscillations in Rg represent a dynamic [6]. The Rg profiles presented here reveal the intermolecular interactions that are responsible for transition from expanded, disordered states to highly packed arrangements that are basis for nucleation. The following data is evident of how single variations in the KLVFFAE sequence can redefine the kinetics of structural organization.

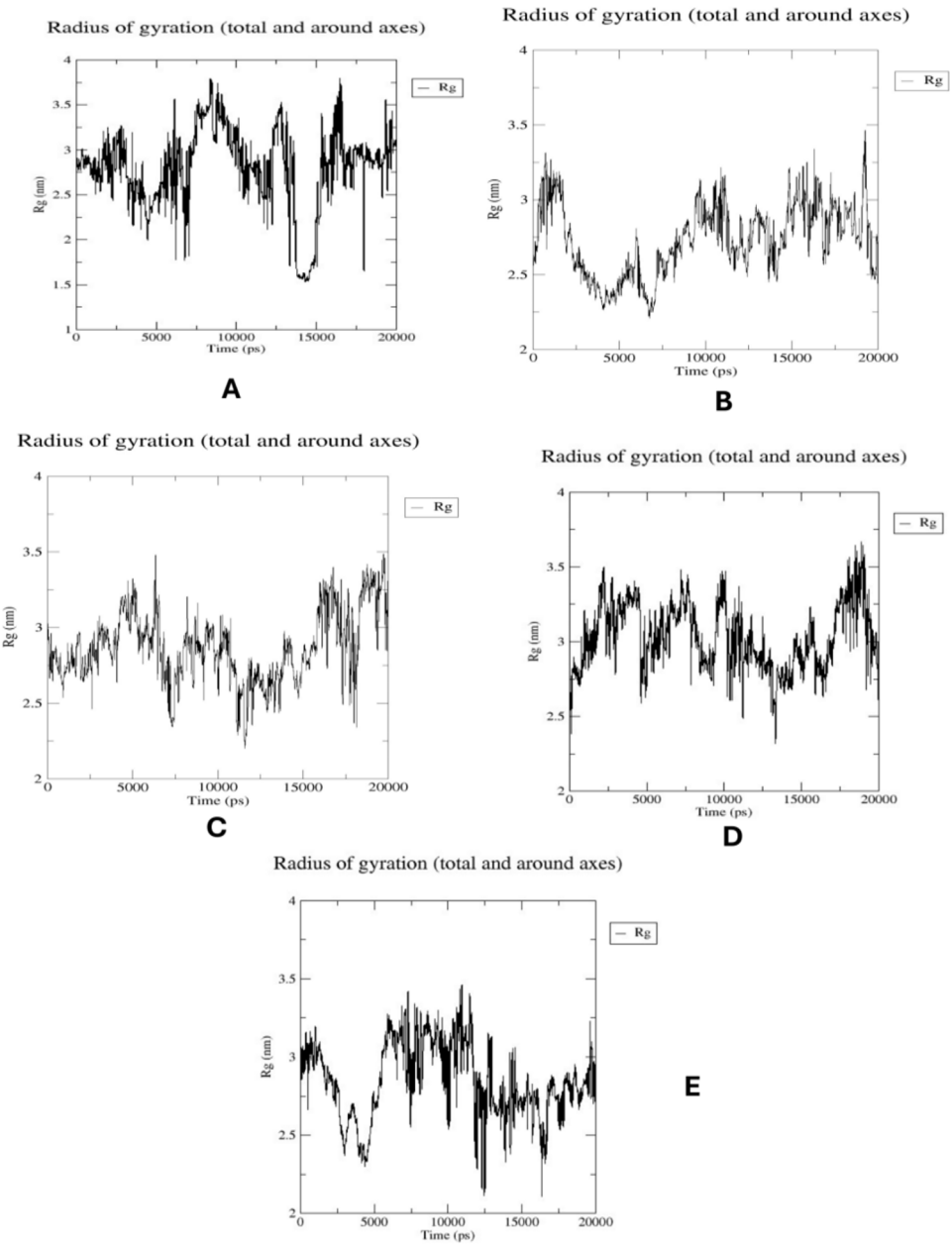

Figure 4(A-E): Radius of gyration (Rg) as a function of time (20 ns) of the peptides 1-5 in 20 ns MD simulations.

Peptide 4 (ALVFFAE) and Peptide 5 (LVFKFAE) are highly compact in nature, which is characteristic of hydrophobic collapse, but Peptide 3 (KLPFFAE) has higher values of Rg, signifying the hindrance of structural packing. These findings indicate that sequence-dependent compactness of oligomers is modulated.

The Rg of hydrophobic-enhanced Peptide 4 (ALVFFAE) showed a gradual decline in Rg, which was replaced by a constant average at a lower value, indicating that the oligomers were rapidly compacting into their required shapes. This is expected of hydrophobic collapse-induced intermolecular association. A similar pattern was observed with Peptide 5 (LVFKFAE) where it was also observed to be reducing substantially in Rg, indicating an ability to effectively pack and stabilize oligomeric assemblies.

Conversely, the proline-containing Peptide 3 (KLPFFAE) shows relatively higher, more oscillatory Rg values, indicating decreased structural compaction. Conformational rigidity caused by proline probably interferes with ordered intermolecular packing. The more positively charged peptide (KKVFFAE) was less compact and showed greater variability, suggesting that electrostatic repulsion, to some degree, prevented hydrophobic association. Peptide 2 (KIVFFAE) showed intermediate behaviour, supporting the hypothesis that β-propensity facilitates structural organization but does not, by itself, facilitate maximal compaction.

Overall, these findings indicate that hydrophobic content and positioning are the key factors influencing oligomeric collapse, whereas charge distribution and backbone constraints dictate compaction efficiency.

Next up we calculated the SASA values of these oligomeric peptides, after MD simulation over 20ns time span. The results were hypothesized to indicate that aggregation prone peptide analogues were to show drop or decrease in SASA values that would mean that they are more prone to hydrophobic clustering thus indicating their potential for hydrophobic collapse.

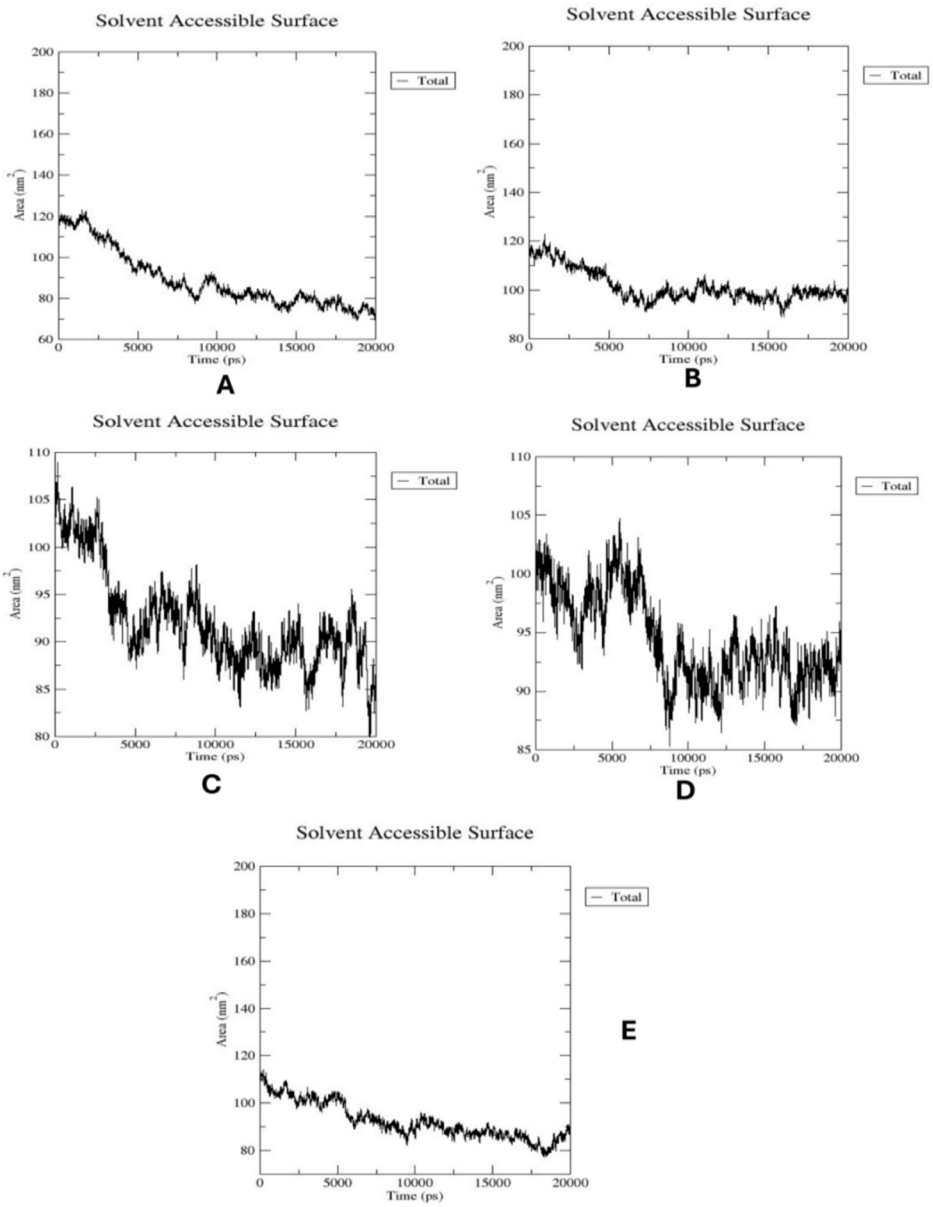

Figure 5: Time evolution of solvent accessible surface area (SASA) for peptide oligomers during 20 ns MD simulations. Peptides with improved hydrophobicity (ALVFFAE and LVFKFAE) exhibit greater SASA changes, suggesting that the hydrophobic residues are buried efficiently and that oligomeric assembly is stabilized. Replacement of proline decreases the efficiency of hydrophobic collapse.

The reduction in SASA was significantly observed in Peptide 4 (ALVFFAE) and was gradual over time, as evidenced by the decrease in Rg. This reduction indicates burial of hydrophobic residues and the solidification of intermolecular contacts. The reduction in SASA was also constant for peptide 5 (LVFKFAE), which implies that the oligomer core was effectively packed with hydrophobic side chains. Peptide 3 (KLPFFAE) registered relatively minor decreases in SASA, indicating that it was partially buried hydrophobically and less organized. The peptide 1 (KKVFFAE) had a greater solvent exposure as compared to the enhancer peptide, which may be a result of the electrostatic repulsion between the lysine residues. The intermediate aggregation was supported by a moderate SASA reduction in peptide 2 (KIVFFAE).

The close association between the reduction of SASA and Rg suggests that hydrophobic interactions are the major force in the early stabilization of oligomers in those peptide systems. Intermolecular hydrogen bonds were also tracked in order to determine the stabilization of oligomeric assemblies. The results from the Hydrogen bond .xvg files also showed that peptides 4 and 2 exhibited hydrogen bond counts above average during simulation, suggesting the formation of stable intermolecular networks.

Taken together, the combined effects of decreases in Rg and SASA and stabilization of intermolecular hydrogen bonds indicate that hydrophobicity and β-propensity modulation via sequence effects directly control the compaction and stabilization dynamics of oligomers at their early stages.

3.3 Visual Analysis

To show the hydrophobic collapse in peptides 4 and 2, here are the VMD visualization pose snapshots at t(ns), indicating the hydrophobic collapse.

Time t(ns)	1ns	~10-15ns	~20ns
peptide 2	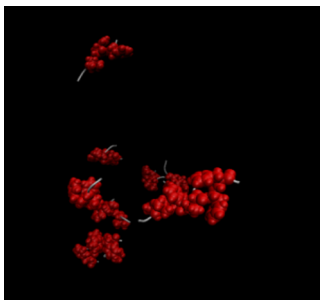	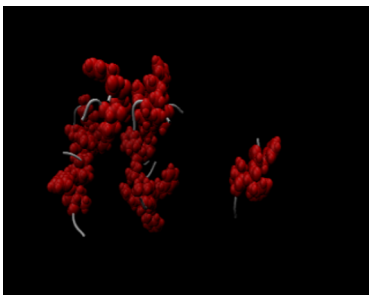	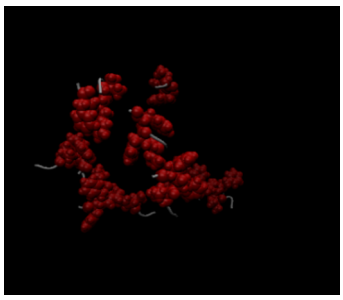
peptide 4	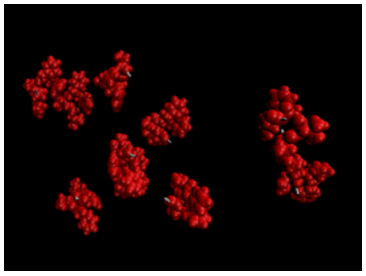	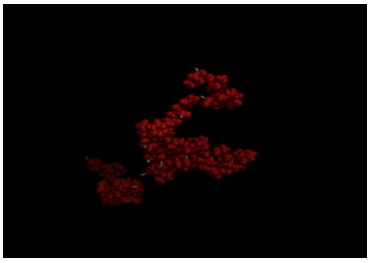	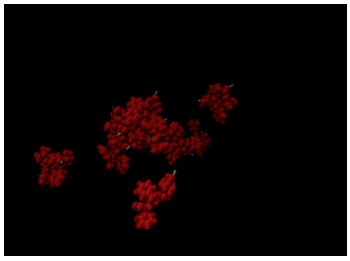

Figure 6: VMD visualisation snapshots illustrating the hydrophobic collapse of peptide 2 and peptide 4 over the course of the MD simulation trajectory at 1 ns, ~10-15 ns, and ~20 ns. VMD input includes clusteredmovie.xtc file loaded onto molecule protein only.gro file. In the graphics, all residues are shown as white (NEWCARTOON), and aggregation-driven hydrophobic residues [peptide 2: I, V, F and peptide 4: L, V, F] are shown in red as Van der Waals spheres.

In the case of Peptide 2 (KIVFFAE), oligomerisation proceeds progressively. At approximately 1 ns, peptide chains are mainly spread out, which is consistent with the increase in SASA and Rg observed in earlier simulation frames. At a timescale of about 10-15 ns, clustering appears as hydrophobic residues (I, V, F) are oriented towards the middle of the assembly, indicating that hydrophobic association occurred gradually. At approximately 20 ns, a small oligomer forms that contains a partially structured hydrophobic core, although the structure still has a relatively high level of conformational flexibility. This activity is consistent with its intermediate decreases in Rg and SASA and an increase in hydrogen bonding, indicating that β-propensity and ordering are favoured but do not achieve optimal compaction.

Peptide 4 (ALVFFAE), on the other hand, exhibits a slower, stronger collapse. Although at first the inter-chain contacts between hydrophobic residues (L, V, F) are dispersed (at approximately 1 ns), they become more pronounced over time, resulting in a compact central core (at about 10-15 ns). At around 20 ns, the oligomer becomes packed and globular, with strong burial of hydrophobic side chains. This visual compression directly supports the more pronounced decrease in Rg, the greater SASA reduction, and the more intense intermolecular hydrogen bonding, as seen quantitatively.

These observations indicate that known models involve hydrophobic interactions to mediate early amyloid collapse prior to β sheet consolidation [11,12].

4. Discussion

Early conformational rearrangements that initiate aggregation of amyloid-β (Aβ) peptides preceded fibril formation and are largely involved in oligomer toxicity [13]. In this case, we examined the regulation of monomer stability and oligomer compaction by intrinsic sequence changes at the Aβ16-22 hot spot (KLVFFAE).

As demonstrated by Chiti and Dobson (2017), aggregation propensity is internally regulated and encoded within the amino acid sequence, with hydrophobicity and β-sheet propensity as the main factors in amyloid formation. Building on this framework, the use of proline substitution in this study supports its role as a beta-strand breaker, leading to suppression of β-structural sampling [11]. These findings validate the notion that significant changes in the primary sequences rearrange the original conformational map of Aβ segments.

Oligomer simulations also show that hydrophobic enhancement brings the biggest changes on radius of gyration and SASA, which denotes effective hydrophobic collapse. Structural ordering (via augmented β-propensity) is made easier, but it is evident that augmented β-propensity, by itself, is ineffective in achieving maximum compaction, and that hydrophobic positioning is a significant factor in the formation of early assemblies. The aggregation behaviour is suppressed by charge enrichment (KKVFFAE) and is consistent with electrostatic repulsion during intermolecular association. In accordance with the mechanistic results proposed by Cremades and Dobson (2018), our results also show a systematic approach to amyloid assembly, wherein hydrophobic interactions initiate early collapse, followed by subsequent stabilization via β-sheet alignment and hydrogen bonding [12].

While previous studies mainly focused on full-length Aβ peptides, the present study adopts a sequence-centric approach by

systematically engineering intrinsic determinants within the Aβ 16-22 hot spot. By showing that modulating the hydrophobicity, β-propensity, or charge within this aggregation-driven core alters early aggregation behaviour, we provide proof that this strategy can serve as a predictive framework for modulating early oligomer assembly.

5. Conclusion

This work establishes the Aβ16-22 segment as a conformational control hotspot whose aggregation behaviour is governed by intrinsic sequence-level determinants. We used a rational peptide design strategy to systematically explore each known physicochemical driver underlying early conformational transitions.

Monomer simulations of our work supported the idea that single-residue substitutions have a major impact on shaping the conformation, altering β-region sampling and structural stability prior to intermolecular association. Whereas our oligomer simulation revealed a hierarchical mechanism of amyloid assembly in which: (i) increased hydrophobicity facilitated rapid hydrophobic collapse and oligomer compaction as indicated by SASA values; (ii) β-propensity enabled structural rearrangement but did not independently maximize aggregation; (iii) proline substitution disrupted β-sheet sampling and suppressed stabilization; and (iv) charge enrichment modulated assembly through electrostatic repulsion as shown by our peptide analogue (KKVFFAE).

Together, these results lead to the conclusion that properties encoded in the primary sequence can be used to predict early aggregation behaviour before it converts into macroscopic fibrils [13,14]. Rather than investigating the full-length Aβ, this motif centred strategy entraps the minimal structural determinants that mediate the conformational switching and oligomeric stabilization.

Importantly, this work provides a computational framework for sequence-focused modulation of aggregation-prone motifs. Future investigations will include employing extended simulation timescales and experimental validation to clarify how these intrinsic determinants scale to full-length Aβ aggregation and neurotoxicity.

6. References

1) Qin Ruixue, Zhao Huijuan, Gao Hui, Liu He. Global trends in Alzheimer's disease and other dementias: A comprehensive analysis of incidence, socio-demographic variations, and future projections. PLOS ONE. 20(12) (2025). doi:10.1371/journal.pone.0338018.

2) N. Cramer, G. Kawecki, K.M. King, D.R. Bevan, A.M. Brown. Insight into Cross Amyloid Interactions and Morphologies: Molecular Dynamics Simulations of Model Peptide Fragments of Amyloid-β (Aβ16-22) and Islet Amyloid Polypeptide (IAPP20-29). bioRxiv, 461861 (2021). doi: https://doi.org/10.1101/2021.09.26.461861.

3) Rojekar S, Gholap AD, Jadhav K et al. Exploring Protein Aggregation in Biological Products: From Mechanistic Understanding to Practical Solutions. AAPS PharmSciTech. 26, 189 (2025). https://doi.org/10.1208/s12249-025-03189- 2.

4) Goyal D, Shuaib S, Mann S, Goyal B. Rationally Designed Peptides and Peptidomimetics as Inhibitors of Amyloid-β (Aβ) Aggregation: Potential Therapeutics of Alzheimer's Disease. ACS Comb Sci. 19, 55-80 (2017). doi: 10.1021/acscombsci.6b00116.

5) Heller GT, Aprile FA, Michaels TCT et al. Small-molecule sequestration of amyloid-β as a drug discovery strategy for Alzheimer's disease. Sci Adv. 6(45) (2020). doi: 10.1126/sciadv.abb5924.

6) Saravanan Konda Mani, Zhang Haiping, Zhang Huiling, Xi Wenhui, Wei Yanjie. On the Conformational Dynamics of β Amyloid Forming Peptides: A Computational Perspective. Frontiers in Bioengineering and Biotechnology. 8, 2296-4185 (2020). doi: 10.3389/fbioe.2020.00532.

7) Roldán-Martín Lorena, Sodupe Mariona, Maréchal Jean-Didier. Computational Study of Amyloidβ42 Familial Mutations and Metal Interaction: Impact on Monomers and Aggregates Dynamical Behaviors. Inorganic Chemistry. 63, 4725-4737 (2024). doi: 10.1021/acs.inorgchem.3c04555.

8) Louros N, Konstantoulea K, De Vleeschouwer M, Ramakers M, Schymkowitz J, Rousseau F. WALTZ-DB 2.0: an updated database containing structural information of experimentally determined amyloid-forming peptides. Nucleic Acids Res. 48, D389-D393 (2020). doi: 10.1093/nar/gkz758.

9) Abraham Mark, Murtola Teemu, Schulz Roland, Páll Szilárd, Smith Jeremy, Hess Berk, Lindahl Erik. GROMACS: High performance molecular simulations through multi-level parallelism from laptops to supercomputers. SoftwareX. 1, 19-25 (2015). doi: 10.1016/j.softx.2015.06.001.

10) Nunia Khushi, Bayen Moushila, Ansary Sahire, Kumar Anupam, Mishra Pankaj. Static and Dynamic Properties of SPC/E Water Model. Journal of Physics: Conference Series. 2663(2023). DOI - 10.1088/1742-6596/2663/1/012037.

11) Chiti F, Dobson CM. Protein Misfolding, Amyloid Formation, and Human Disease: A Summary of Progress Over the Last Decade. Annu Rev Biochem. 86:27-68 (2017). doi: 10.1146/annurev-biochem-061516-045115.

12) Cremades N, Dobson CM. The contribution of biophysical and structural studies of protein self-assembly to the design of therapeutic strategies for amyloid diseases. Neurobiol Dis. 109:178-190 (2018). doi: 10.1016/j.nbd.2017.07.009.

13) Walsh DM, Selkoe DJ. Amyloid β-protein and beyond: the path forward in Alzheimer's disease. Curr Opin Neurobiol. 61:116-124 (2020). doi: 10.1016/j.conb.2020.02.003.

14) Knowles TP, Vendruscolo M, Dobson CM. The amyloid state and its association with protein misfolding diseases. Nat Rev Mol Cell Biol. 15:384-96 (2014). doi: 10.1038/nrm3810.